I&EC research
Industrial & Engineering Chemistry Research

ARTICLE

pubs.acs.org/IECR

Influence of Large Obstacles and Mitigation Barriers on Heavy Gas Cloud Dispersion: a Liquefied Natural Gas Case-Study

Valentina Busini, Massimiliano Lino, and Renato Rota*

Dipartimento di Chimica, Materiali e Ingegneria Chimica "Giulio Natta", Politecnico di Milano, via Mancinelli 7, 20131 Milano, Italy

ABSTRACT: The study of the consequences of heavy gases releases is of paramount importance in the safety analysis because of the large damage areas involved. The Computational Fluid Dynamics (CFD) models, unlike the integral ones that are simpler and faster, allow for a complete description of complex geometries, such as those involved in industrial plants or urban areas. In this work, the effect of typical large obstacles present in a real plant has been studied. Moreover, to verify the effectiveness of mitigation barriers on the dispersion of clouds produced by massive release of heavy gases, several types of walls have been investigated by analyzing the induced changes in the hazardous area.

1. INTRODUCTION

In risk analysis studies, modeling the consequences of gaseous material (toxic or flammable) releases in the atmosphere plays a central role, as they can lead to several types of adverse effects on the public health, including fires and explosions. Particular attention is required when the released gas is heavier than air, as this results in larger hazardous areas.[1]

Since the 1970s, experimental campaigns have been carried out on open-field releases of dense gases and several modeling tools have been developed.[2−4] Moreover, considering that the tests involving hydrocarbon mixtures, such as Liquefied Natural Gas (LNG), are expensive and difficult to carry out, because they require very large areas far from inhabited places, several data come from laboratory tests, such as the wind tunnel ones.[5,6]

Nowadays, the main difficulties encountered in atmospheric dispersion studies are related to the presence of large obstacles within the area affected by the release of dense gas. Several mathematical models have been developed for simulating heavy gas dispersion in the atmosphere,[7,8] and they are classified into three categories of increasing complexity: specific models, integral models, and three-dimensional models.[9] It is well-known that the first two classes of models cannot correctly represent dense gas dispersion in the presence of large obstacles, such as those present in many plants and in urban areas close to them.[10] Moreover, large obstacles are intrinsically present when containment walls are built for damage mitigation.

On the other hand, three-dimensional models developed in the frame of the Computational Fluid Dynamics (CFD) have been successfully validated against experimental real−scale field data[11−14] and lab-scale trials,[15,16] thus even exploiting the geometries of realistic urban areas.[17−19] CFD methods implement on a spatial domain, reproduced by a suitable computational grid, the basic equations of conservation of mass, energy, and momentum, along with turbulence models and well-defined boundary conditions. In recent years the amount of scientific publications in this field has been considerably boosted, with proof of the interest held by this sector of science. The weakness of these models is the considerable computational effort required.

Consequently, the use of CFD tools should be restricted to cases significantly influenced by the geometry: in other words, using integral models in geometrically complex environments can lead to wrong estimates of the risk area; whereas using a CFD approach in the presence of simple geometries can lead to a waste of resources.

Therefore, the aim of this work was 2-fold: to study the effect of the typical large obstacles of a realistic industrial plant geometry on heavy gas dispersion and to verify the effectiveness of some type of containment walls as damage mitigation works on the dispersion of clouds produced by the massive release of dense gas.

2. THEORETICAL BACKGROUND

Computational fluid dynamics codes numerically solve the equations of motion, discretizing the domain through the use of a calculation grid, called *mesh*, and transforming the mathematical problem from a system of partial differential equations to a system of algebraic equations. Along with Navier−Stokes eqs 1 and 2, CFD codes solve specific model equations, such as those arising from energy balance (eq 3) and turbulence modeling.[20]

$$\frac{\partial \rho}{\partial t} + \nabla \cdot (\rho \vec{v}) = 0 \tag{1}$$

$$\frac{\partial (\rho \vec{v})}{\partial t} + \nabla \cdot (\rho \vec{v}\vec{v}) = -\nabla p + \nabla \cdot (\bar{\bar{\tau}}) + \rho \vec{g} \tag{2}$$

$$\frac{\partial (\rho c_v T)}{\partial t} + \nabla \cdot (\rho \vec{v} c_p T) = \nabla \cdot (k_T \nabla T) \tag{3}$$

In the equation just cited, ρ is the density, t is the time, v is the velocity, p is the pressure, τ is the shear stress, g *is* the acceleration of gravity, c_v and c_p are the specific heats, T is the temperature, and k_T is the thermal conductivity.

Special Issue: Russo Issue

Received: July 22, 2011
Accepted: December 21, 2011
Revised: November 19, 2011
Published: December 21, 2011

dx.doi.org/10.1021/ie201591b | *Ind. Eng. Chem. Res.* 2012, 51, 7643–7650

In this work the k−ε model was used for representing the effects of the turbulence. This model introduces two additional transport equations for turbulent kinetic energy k (eq 4) and turbulent kinetic energy dissipation rate ε (eq 5), respectively:[21]

$$\frac{\partial(\rho k)}{\partial t} + \frac{\partial(\rho k v_i)}{\partial x_i} = \frac{\partial}{\partial x_j}\left[\left(\mu + \frac{\mu_t}{\sigma_k}\right)\frac{\partial k}{\partial x_j}\right] + G_k + G_b - \rho\varepsilon - Y_M + S_k \quad (4)$$

$$\frac{\partial(\rho \varepsilon)}{\partial t} + \frac{\partial(\rho \varepsilon v_i)}{\partial x_i} = \frac{\partial}{\partial x_j}\left[\left(\mu + \frac{\mu_t}{\sigma_\varepsilon}\right)\frac{\partial \varepsilon}{\partial x_j}\right] + C_{\varepsilon 1}\frac{\varepsilon}{k}(G_k + C_{\varepsilon 3}G_b) - C_{\varepsilon 2}\rho\frac{\varepsilon^2}{k} + S_\delta \quad (5)$$

where v_i is the velocity component along x_i direction, μ is the viscosity, μ_t is the turbulent viscosity, G_k is the shear stress-related turbulent kinetic energy production, G_b is the buoyancy−related turbulent kinetic energy production, Y_M is the compressibility-related kinetic energy production and S_k and S_ε are user-defined source terms.

$C_{\varepsilon 1}$, $C_{\varepsilon 2}$, $C_{\varepsilon 3}$, σ_k, σ_ε, and C_μ are empirical constants; in this work, Jones and Launder[22] values have been used.

The k−ε turbulence model was complemented with an Atmospheric Stability sub-Model, called *ASsM*,[23] which is able to ensure the consistency of the CFD results with the Monin−Obukhov theory,[24] by introducing a user−defined source term S_ε defined as (for neutral conditions):

$$S_\varepsilon(Z) = \rho\frac{u_*^4}{Z^2}\left[\frac{(C_{\varepsilon 2} - C_{\varepsilon 1})\sqrt{C_\mu}}{K^2} - \frac{1}{\sigma_\varepsilon}\right] - \mu\frac{2u_*^3}{Kz^3} \quad (6)$$

Moreover, for the ground boundary conditions, the ASsM model uses a roughness constant, C_s, equal to 0.979 in the wall functions, and a surface shear stress, τ_w.

The commercial package Fluent 12.1.2[25,26] was used for all the computations, together with the boundary conditions summarized in Table 1.

Moreover, for the sake of comparison the Process Hazard Analysis Software Tools (PHAST) software was also used;[27] PHAST can examine the progress of a potential accident from the initial release to the far-field dispersion including modeling of pool spreading and evaporation through integral models, which are unable to account for the presence of large obstacles as previously discussed.

3. ACCIDENTAL SCENARIO SETUP

3.1. Characterization of the Accidental Scenario. As a case study, a release of LNG in a typical regasification terminal was selected because of both the large amount of fluid stored and the presence of several obstacles with a significant size.

In fact, a typical configuration of an LNG terminal[28] includes a jetty for mooring of LNG carriers, a pipeline to transport LNG from ships to tanks for the storage of LNG, a pumping unit, a group of evaporators for the intake of LNG in the distribution network, and several other minor items, such as a torch and several piping sections. Therefore, the layout of these plants is quite complex, and it would be a waste of resources and CPU time to fully represent it in a CFD simulation model as it would require a very large number of cells and, consequently, a huge amount of computational resources and CPU time. This means

Table 1. Boundary Conditions

ground	wall, roughness =0.06 m
buildings and walls	adiabatic wall
pool	during the atmospheric stabilization: wall @ 300 K, roughness = 0.06 m
	during the pool evaporation: mass flow inlet
	after the end of the pool evaporation: adiabatic wall
wind inlet, domain sides, sky	velocity inlet
wind outlet	pressure outlet

that a simplified geometry, containing all the most important elements, without being too detailed, to be simulated within the limits imposed by available computational power, should be identified. In fact, the presence of very different sizes requires the construction of a locally dense mesh (where there are small obstacles), thus causing a sharp increase in the number of equations and therefore of the computational power required. On the other hand, it is expected that small obstacles will only marginally affect the hazardous distance.

In this regard, a criterion to identify when an obstacle is able to significantly modify the cloud dispersion with regard to that expected in a free field scenario has been proposed, with the aim of discriminating the situation where an integral model can be safely used to those where a CFD approach is required.[29] Such a criterion can be also used for the simplification of the geometry to identify which obstacles are not expected to play a relevant role in cloud dispersion. In particular, a dimensionless parameter R^* allows the characterization of different types of obstacle. Such a parameter is defined as the minimum between the ratios of the obstacle frontal face height, h_{obs} (or width, w_{obs}), to the cloud height, h_{cld} (or width, w_{cld}) evaluated without the obstacle:

$$R_h = \frac{h_{obs}}{h_{cld}} \quad (7)$$

$$R_w = \frac{w_{obs}}{w_{cld}} \quad (8)$$

$$R^* = \min(R_h, R_w) \quad (9)$$

It has been shown[29] that for $R^* < 0.25$ the obstacle influence can be disregarded, whereas for $R^* > 1$ it cannot be disregarded.

However, to use this criterion it is necessary to estimate the characteristic cloud dimension in open−field conditions (that is, without any obstacle). This requires defining an accidental scenario, which was assumed as originating from the breaking of a large LNG pipeline forming an evaporating pool. The characteristic dimensions of the unsteady state cloud arising from the pool were computed (in open-field conditions) by using the PHAST suite of program, and it was used to estimate the R^* value for the typical obstacles present in an LNG regasification plant; this leads to disregarding the exchangers group ($R^* = 0.2$), the pipelines ($R^* \ll 1$), and the flare ($R^* \ll 1$). Therefore, the assumed configuration involves two large tanks (diameter 80 m and height 62.4 m) for LNG storage downwind from the pool, a series of smaller tanks (diameter 40 m and height 20 m) on the sides, and some buildings and equipment upwind from the pool.

The release of LNG was assumed from a part of the plant placed at a distance from the jetty sufficient to disregard this structure and the interaction of LNG released with seawater since

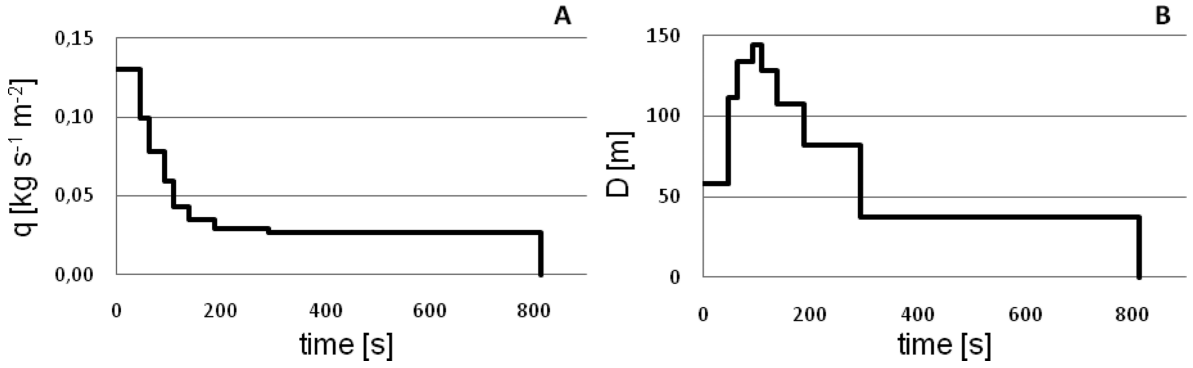

Figure 1. Source term computed with PHAST and used in the CFD simulations. (A) specific mass flow rate from the pool; (B) pool diameter.

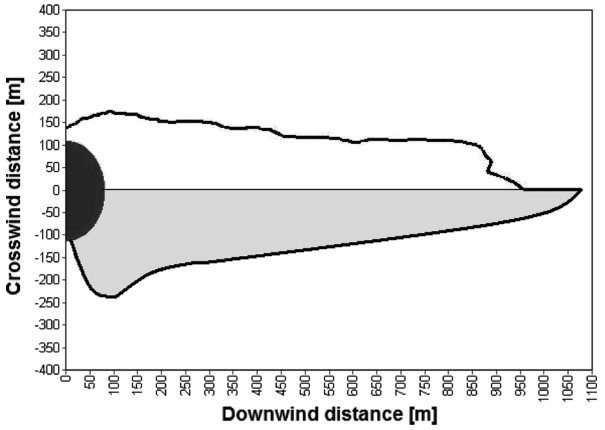

Figure 2. Comparison between the CFD model (up) and the integral model (down) predictions in open-field for the hazardous (LNG concentration > LFL/2) region.

considering the interactions with seawater would significantly complicate the description of the accidental scenario. In fact, for the release of LNG on water it is also important to consider the transfer of water and heat from the substrate; in addition, usually the presence of water dilutes and heats the cloud, leading to a decrease of the distance at which it reaches the lower flammability limit, as confirmed by some recent investigations.[30−32]

3.2. Open-Field Simulations. As previously mentioned, the chosen scenario was modeled with the software PHAST, neglecting any obstacle or basin to contain the dimension of the pool. The results of this simulation in terms of specific mass flow rate evaporating from the pool and pool diameter are shown in Figure 1A and 1B, respectively.

The lower part of Figure 2 illustrates the maximum distance at which the LNG concentration reaches values higher than LFL/2 (half of Lower Flammability Limit), according to PHAST predictions with neutral (D) stability class and 5 m/s wind speed at 2 m above the ground. It is not representative of a specific time after the start of the release, but it shows the area where hazardous concentration values larger than LFL/2 are expected. According to Figure 2, PHAST predicts that the cloud takes the typical elongated shape of dense gas releases, with a fair spreading in the initial part (about 500 m in the widest section, at about 100 m downwind of the center of the pool) and a progressive narrowing up to dissipation; the maximum distance reached by the cloud is located at about 1070 m from the center of the pool.

Table 2. Grid Independence Analysis for Both the Open-Field and the Case Study

number of cells	LFL/2 m
Open-Field	
1.2×10^6	1000
1.6×10^6	950
2.8×10^6	950
Case Study	
5.7×10^6	430
9.3×10^6	425

These results are expected to be reliable in the absence of large obstacles since PHAST has been successfully validated for comparison with experimental data obtained in the open-field.[27]

These results obtained from the integral model were compared with the CFD simulation in open-field. For the construction of the mesh GAMBIT[33] size functions were used to make the grid denser in the critical areas. Furthermore, a boundary layer was created on the ground, which was composed of two rows of prismatic cells (for an overall height of 24 cm), for a better modeling of the surface roughness.[34] The size of the domain of integration for the open-field case was 2000 × 100 × 1200 m.

The pool obtained with PHAST was used as the only source term of natural gas, and its time behavior, shown in Figure 1, was represented in the CFD simulations using eight concentric circular surfaces. To simulate the initial expansion and the subsequent shrinkage of the pool, the boundary conditions of those surfaces, initially set as *wall* with the same characteristic of the terrain (during the first phase of wind stabilization), were gradually changed to *mass flow inlet* and then switched to *adiabatic walls*.

All the simulations were carried out assuming a neutral stability class (D), characterized by a wind speed of 5 m/s at a reference height of 2 m above the ground; this allows the creation of profiles of u, k, and ε at the wind inlet accordingly with the Monin−Obukhov theory.[24] Moreover, air temperature was set at 300 K and adiabatic conditions were set at the surfaces characterized by wall type boundary condition.

The upper part of Figure 2 is the projections of the LFL/2 contour on the ground predicted by the CFD model. The grid independence was checked with three different meshes ($1.2\ 10^6$, $1.6\ 10^6$ and $2.8\ 10^6$ cells), as shown in Table 2, the results obtained in terms of maximum hazardous distance are comparable. As for the PHAST simulation, the cloud develops mainly

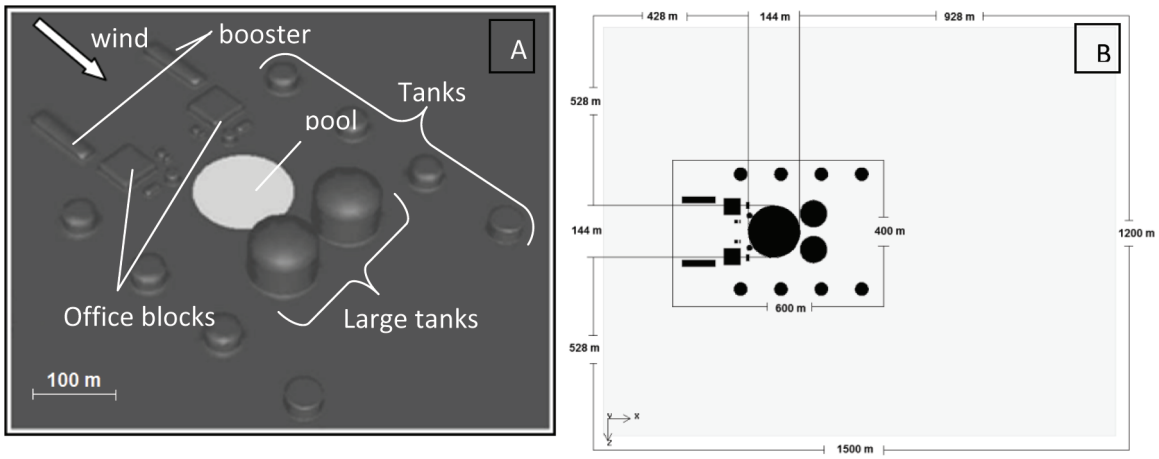

Figure 3. (A) Geometric configuration and (B) integration domain for the considered case-study.

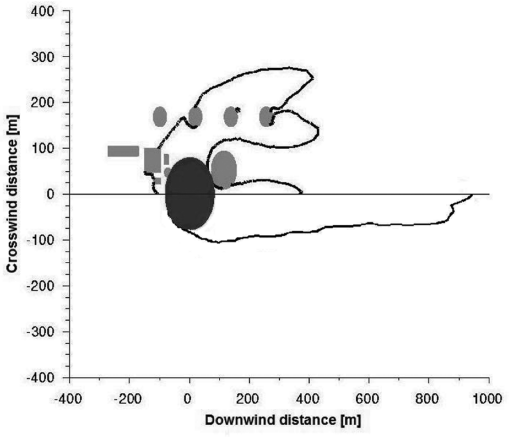

Figure 4. Comparison between the considered case-study (up) and the open-field (down) predictions for the maximum LFL/2 footprint. Black areas represents the pool; gray areas represents the building.

along wind direction, even if the spreading is less significant (about 300 m in the widest section, at about 100 m from the center of the pool) and the narrowing takes place more gradually, thus leading to a more abrupt end of the cloud. The maximum distance reached by the cloud is about 950 m from the center of the pool.

From Figure 2, we can see that, for open-field conditions, the results obtained by CFD are quite close to PHAST predictions in terms of the maximum LFL/2 distance. The CFD model predicts a slightly lower LFL/2 distance; this is coherent with the findings of Pitblado et al.,[35] who reported that PHAST usually over predicts the experimental data concerning LNG dispersion.

4. RESULTS AND DISCUSSION

4.1. Obstacles Effect. The effect of the presence of large obstacles on the cloud dispersion was assessed by comparing the results of the CFD model in the open-field discussed in the previous section with those obtained for the aforementioned case study. Obviously, the presence of obstacles does not change the PHAST predictions, because integral models cannot account for the presence of large three-dimensional obstacles.

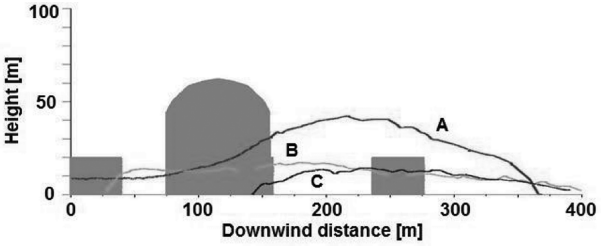

Figure 5. Cloud height profile at LFL/2 along wind direction. A, domain symmetry plane; B, plane at 150 m crosswind; C, plane at 250 m crosswind. Gray areas represent the tanks' position.

The integration domain (1500 × 150 × 1200 m) used for the case-study is shown along with pool and obstacles in Figure 3.

The CFD model results are summarized in the upper part of Figure 4 in terms of maximum LFL/2 footprint at the ground level. Also in this case the grid independence was checked with two different meshes ($5.7\ 10^6$ cells and $9.3\ 10^6$ cells), as shown in Table 2. It can be clearly seen that the maximum distance at the ground reached by the LFL/2 concentration is greatly reduced in the presence of large obstacles from 950 to 430 m. This behavior is due to the increasing turbulent phenomena and the resulting changes in the flow field generated by the obstacles. We can also see how the presence of buildings (especially of the two larger tanks) leads to a channeling of the cloud, thus creating preferential directions of the cloud dispersion. Furthermore, the presence of obstacles also acts on the cloud height as can be seen in Figure 5 showing the LFL/2 profiles of the cloud along the wind direction for three vertical planes, located at the symmetry plane of the domain (curve A) and at distances 150 and 250 m crosswind from the cloud axis respectively (curves B and C). These three planes correspond to the tips of the cloud, as shown in Figure 4. On the symmetry plane the cloud reaches heights much greater than in the lateral zones, until a maximum of about 40 m at about 200 m from the pool center, which is just behind the two larger tanks. Laterally, the height of the cloud always remains below 20 m.

Accordingly with the general criterion discussed elsewhere,[29] the influence of large obstacles is definitely not negligible, thus leading to more than halving the damage distance in comparison to the open-field predictions; this confirms the need to use

CFD methods when studying geometrically congested industrial sites to obtain meaningful results. However, it should also be mentioned that, as expected, the usual integral models lead to conservative results. This is a welcomed feature when performing safety analysis, even if it can lead to a large waste of resources.

4.2. Effectiveness of Mitigation Barriers. The third series of simulations carried out with the CFD model was aimed at verifying the effectiveness of passive protection measures.

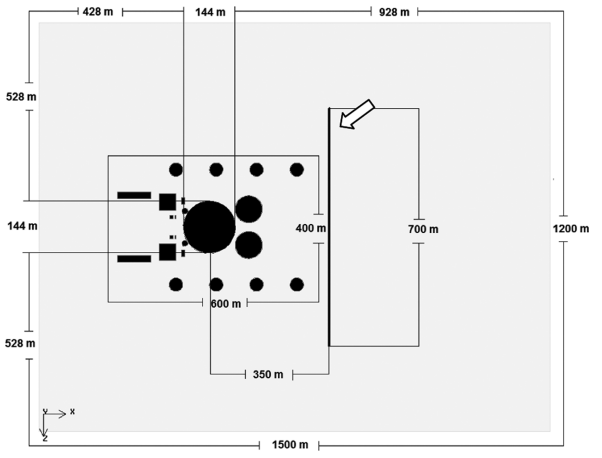

Figure 6. Integration domain for the considered case-study with the addition of the mitigation barrier. The arrow indicates the mitigation barriers.

In particular, once established that the presence of obstacles of a significant size changes the damage distance (defined by the maximum LFL/2 cloud boundary), it was investigated whether the presence of a containment wall with proper dimensions can further reduce the damage distance. This was done by comparing the previously discussed CFD results for the case study investigated with those obtained by simulating the same configuration with the addition of a containment wall located 350 m far from the pool center.

Such a distance allows the wall to be located outside the tanks zone. As shown in Figure 6, the barrier is 700 m wide (symmetrical to the central axis) to thoroughly contain the entire width of the cloud. The thickness of the barrier (0.5 m) does not require to highly thicken the mesh near the wall. The criterion discussed elsewhere[29] in essence states that an obstacle strongly influences the cloud dispersion only when its characteristic dimensions are comparable with the characteristic dimensions of the cloud without the obstacle (see eqs 7 to 9). This means that the wall height should be close to 12 m ($R^* = 1$), as can be deduced from the cloud height at 350 m shown in Figure 5.

The maximum LFL/2 footprint of the cloud in this configuration is shown in Figure 7A. The effect of the wall is to initially hinder the movement of the cloud in the wind direction, thus modifying its lateral dispersion. Subsequently, the cloud overtakes the wall that increases the mixing of the cloud with the atmosphere, thereby reducing the damage distance up to 350 m. In other words, the barrier completely blocks the cloud, thus

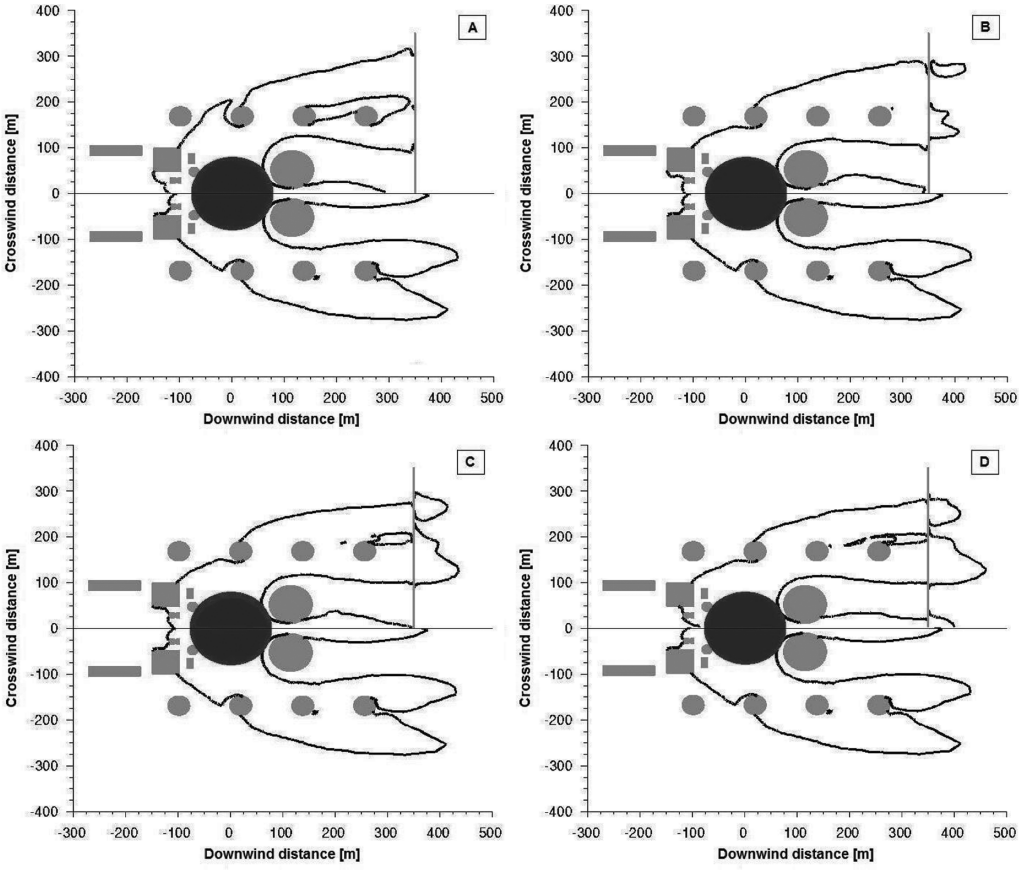

Figure 7. Comparison between the considered case-study (down) and the configuration with mitigation barriers (up) predictions for the maximum LFL/2 footprint. (A) 12 m-high wall; (B) 9 m-high wall; (C) 6 m-high wall; (D) 3 m-high wall. Black areas represent the pool; gray areas represent the buildings; gray lines represent the wall.

dx.doi.org/10.1021/ie201591b |*Ind. Eng. Chem. Res.* 2012, 51, 7643–7650

limiting the damage distance at the wall position, that is, about 19% less than the configuration without the wall.

Provided that a 12 m high barrier can work properly, a sensitivity analysis that focused on the height of the barrier has been carried out. The height of the wall was reduced from the original 12 m to 9, 6, and 3 m, respectively. The results obtained, as usual in terms of maximum LFL/2 footprint, are shown in Figures 7B, 7C, and 7D, respectively, and summarized in Table 3 also in terms of R^* values.

It can be observed that with a 12 m high wall the front of the cloud extends over all the 700 m of the wall width, thus proving that such a width was needed. With the walls with height lower than 12 m, the shape of the cloud remains substantially the same, but the smaller the wall, the more LNG can overtake the barrier, especially sideways. In particular, with the 9 m wall there is a small overcoming of the wall, with immediate fall-out of LNG on the ground, bringing back the maximum damage distance almost to the same value of that of the configuration without the wall. With the 6 and 3 m walls the distance reached tends even to increase with regard to the configuration without the wall. This highlights the presence of a "springboard effect": if the wall is too small compared with the cloud height, it does not lead to significant benefits in terms of turbulence increase, while helping the cloud to rise with the overall effect of extending the maximum damage distance downwind.

The last series of simulations performed was aimed at testing the effect of a different choice for the position of the mitigation barrier, based on the observation of the geometry investigated and on the feasibility of the proposed measures.

Two types of solutions have been investigated, as shown in Figures 8. Configuration A consists of a 12 m-high wall placed at 200 m from the pool center: such barrier has the same height of the wall used in one of the previous simulations at 350 m, but it was moved to the distance corresponding to the maximum height

Table 3. Damage Distances for Mitigation Barriers Located at 350 m with Different Height, Compared with Basic Case-Study, and the Corresponding R* Value

# simulation	LFL/2 from the pool center, m	percentage variation	R^*
case-study	430		
wall 12 m	350	−19%	1
wall 9 m	425	−1%	0.75
wall 6 m	450	+5%	0.5
wall 3 m	465	+8%	0.25

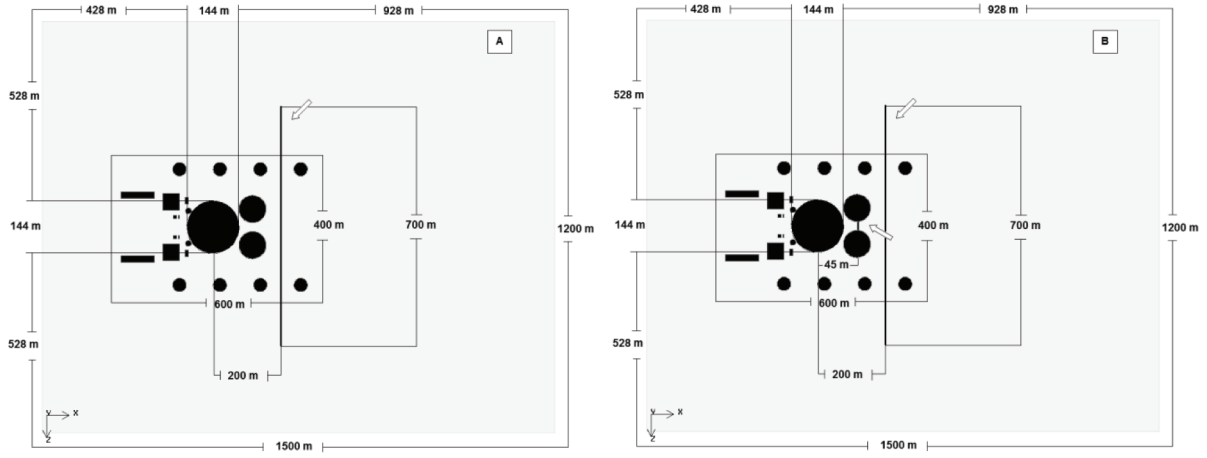

Figure 8. Integration domains for the considered case-study with the addition of a mitigation barrier in two different configurations. The arrows indicate the mitigation barriers.

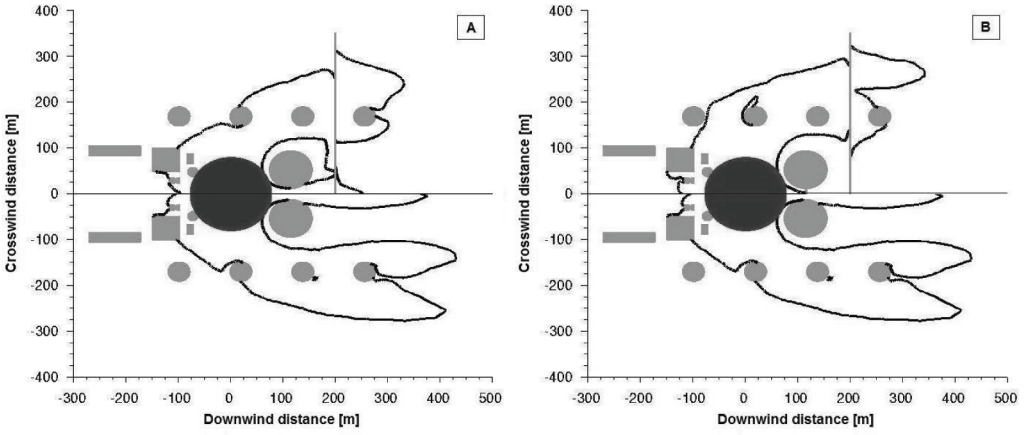

Figure 9. Comparison between the maximum LFL/2 footprint for the considered case-study (down) and two different configurations with the addition of mitigation barriers (up): (A) one 12 m high wall at 200 m; (B) one 12 m high wall at 200 m plus one one 45 m high wall between the two large tanks; black areas represent the pool; gray areas) represent the buildings; gray lines represent the wall.

Table 4. Damage Distances for Different Mitigation Barriers Compared with Basic Case-Study

# simulation	LFL/2 from the pool center [m]	LFL/2 from the barrier, m
case-study	430	
wall 12 m high at 350 m	350	0
wall 12 m high at 200 m (A)	340	140
wall 12 m high at 200 m (B)	350	150

of the cloud as shown in Figure 5. In this position the wall height is slightly lower than the height of the two lateral branches of the cloud ($R^* = 0.9$), whereas it is much lower than the height of the cloud centerline($R^* = 0.3$). Configuration B adds to the wall of the Configuration A another 45 m-high barrier at 110 m from the pool center, in between the two largest tanks to avoid the cloud channeling between the two tanks. The 45 m-high wall was introduced according to the maximum height reached by the cloud and choosing an advantageous position by a construction point of view. The aim was to stop the centerline plume that shows the largest height.

The results obtained are shown in Figures 9 and summarized in Table 4. The 12 m-high wall at 200 m is overtaken in both the central and the side areas, where the cloud reaches a distance of about 340 m; in the Configuration B the central channeling is avoided, but the maximum damage distance obtained is still about 350 m since the cloud overcomes the wall in the side areas. These values are in both cases very similar to those seen for the 12 m-high wall placed at 350 m: this behavior can be explained noting that even at 200 m, the height of the cloud is slightly lower than that of the wall everywhere but on the centerline (see Figure 5). The 45 m-high wall effectively blocks the cloud along the centerline, but it is not in the centerline where the maximum damage distance is reached. However, although the passage of the methane between the two tanks is entirely prevented, the cloud moves toward the lateral zones, thus increasing the cloud extension on the sides. This leads to a slight increase of the damage distance in spite of the addition of a very high mitigation barrier on the centerline. Moreover, considering the distance of the LFL/2 boundary downwind of the wall, it can be seen that the wall at 350 m ($R^* = 1$) is able to completely hinder the cloud (the maximum distance of the LFL/2 boundary downwind the wall is zero), whereas for the barriers at 200 m ($R^* = 0.3$) the cloud overcomes the wall reaching a distance of about 150 m downwind of the wall.

5. CONCLUSIONS

The aim of this work was to study the influence of large obstacles and mitigation barriers on the dispersion of heavy gas clouds. The large obstacles involved in a LNG terminal were used as a case study, since they produce a geometry complex enough to be representative.

It has been found that large obstacles influence cloud dispersion reducing the damage distance more than 50% compared with an open-field release. Such a reduction is larger than the uncertainties related to numerical errors of a typical CFD simulation.

The results on the effectiveness of passive protection measures indicate that height and position of the wall have a great importance and are strongly related to the cloud dimensions in open-field. These results also provide a validation of the criterion discussed elsewhere[29] for predicting when an obstacle can influence the cloud dispersion. As long as the wall has an adequate width, only a wall of the same height of the cloud is able to induce significant variations of the maximum damage distance. Moreover, these results also highlights that a mitigation barrier should be correctly designed, as its location and height are strongly related to the cloud characteristic dimensions without any barriers at that location. It was found that a mitigation barrier can influence the cloud behavior both positively and negatively; this means that it is not sufficient to build up a mitigation barrier, but it should be correctly designed, in terms of both location and height, to be effective in mitigating the accident consequences.

Finally, it is worth mentioning that all the aforementioned conclusions have been derived from the considered case study. Although the case study was chosen so as to be representative of a typical industrial plant involving large obstacles, obvious caution should be taken into account in extending such conclusions to other situations.

AUTHOR INFORMATION

Corresponding Author

*E-mail: renato.rota@polimi.it. Fax. +39 02 2399 3180.

ACKNOWLEDGMENT

The research leading to these results has received funding from the European Union's Seventh Framework Programme (FP7/2007-2013) under grant agreement no. 213345. The authors gratefully acknowledge D'Appolonia SpA HSE Division (Milano, Italy) for providing information related to typical regasification plants.

REFERENCES

(1) Koopman, R. P.; Ermak, D. L. Lessons learned from LNG safety research. *J. Hazard. Mater.* **2006**, *140*, 412.

(2) Bernatik, A.; Libisova, M. Loss prevention in heavy industry: risk assessment of large gasholders. *J. Loss Prev. Process Ind.* **2004**, *17*, 271.

(3) Luketa-Hanlin, A. A review of large-scale LNG spills: Experiments and modeling. *J. Hazard. Mater.* **2006**, *132*, 119.

(4) Middha, P.; Hansen, O. R.; Storvik, I. E. Validation of CFD-model for hydrogen dispersion. *J. Loss Prev. Process Ind.* **2009**, *22*, 1034.

(5) Snyder, W. H. Some observations of the influences of stratification on diffusion in building wakes. In *Stably Stratified Flows: Flow and Dispersion over Topography*; Clarendon Press: Oxford, 1994; p 301.

(6) Ohba, R.; Kouchi, A.; Hara, T.; Vieillard, V.; Nedelka, D. Validation of heavy and light gas dispersion models for the safety analysis of LNG tank. *J. Loss Prev. Process Ind.* **2004**, *17*, 325.

(7) Olvera, H. A.; Choudhuri, A. R.; Li, W. W. Effects of plume buoyancy and momentum on the near-wake flow structure and dispersion behind an idealized building. *J. Wind Eng. Ind. Aerodyn.* **2008**, *96*, 209.

(8) Neofytou, P.; Venetsanos, A. G.; Vlachogiannis, D.; Bartzis, J. G.; Scaperdas, A. CFD simulation of the wind environment around an airport terminal building. *Environ. Modell. Softw.* **2006**, *21*, 520.

(9) Lees, F. *Loss prevention in the process industries, Hazard Identification, Assessment and Control*; Butter-worths/Heinemann: Oxford, U.K., 1996; Vol. 15, p 223.

(10) Landucci, G.; Tugnoli, A.; Busini, V.; Derudi, M.; Rota, R.; Cozzani, V. The Viareggio LPG accident: lessons learnt. *J. Loss Prevention Proc. Ind.* **2011**, *24*, 466.

(11) Nielsen, M., Ott, S. A collection of data from dense gas experiments, RISO Report R-845(EN); RISO: Roskilde, Denmark, 1996.

(12) Sklavounos, S.; Rigas, F. Simulation of Coyote series trials, part I: CFD estimation of non-isothermal LNG releases and comparison with box-model predictions. *Chem. Eng. Sci.* **2006**, *61*, 1434.

(13) Cormier, B. R.; Qi, R.; Yun, G. W.; Zhang, Y.; Mannan, M. S. Application of computational fluid dynamics for LNG vapor dispersion modeling: a study of key parameters. *J. Loss Prev. Process Ind.* **2009**, *22*, 332.

(14) Gavelli, F.; Chernovsky, M. K.; Bullister, E.; Kytomaa, H. Modeling of LNG spills into trenches. *J. Hazard. Mater.* **2010**, *180*, 332.

(15) McBride, M. A.; Reever, A. B.; Vanderheyden, M. D.; Lea, C. J.; Zhou, X. X. Use of advanced techniques to model the dispersion of chlorine in complex terrain. *Proc. Safety Environ. Prot.* **2001**, *79*, 89.

(16) Hanna, S. R., Britter, R. Wind flow and vapor cloud dispersion at industrial and urban sites; CCPS: New York, 2002.

(17) Pontiggia, M.; Derudi, M.; Alba, M.; Scaioni, M.; Rota, R. Hazardous gas releases in urban areas: assessment of consequences through CFD modeling. *J. Hazard. Mater.* **2010**, *176*, 589.

(18) Pontiggia, M.; Landucci, G.; Busini, V.; Derudi, M.; Alba, M.; Scaioni, M.; Bonvicini, S.; Cozzani, V.; Rota, R. CFD model simulation of LPG dispersion in urban areas. *Atmos. Environ.* **2011**, *45*, 3913.

(19) Hanna, S. R.; Hansen, O. R.; Ichard, M.; Strimaitis, D. CFD model simulation of dispersion from chlorine railcar releases in industrial and urban areas. *Atmos. Environ.* **2009**, *43*, 262.

(20) Luketa-Hanlin, A.; Koopman, R. P.; Ermak, D. L. On the application of computational fluid dynamics codes for liquefied natural gas dispersion. *J. Hazard. Mater.* **2007**, *140*, 504.

(21) Hargreaves, D. M.; Wright, N. G. On the use of the k−ε model in commercial CFD software to model the neutral atmospheric boundary layer. *J. Wind Eng. Ind. Aerodyn.* **2007**, *95*, 355.

(22) Jones, W. P.; Launder, B. E. The prediction of laminarization with a two-equation model of turbulence. *J. Heat Mass Transfer* **1972**, *15*, 301.

(23) Pontiggia, M.; Derudi, M.; Busini, V.; Rota, R. Hazardous gas dispersion: a CFD model accounting for atmospheric stability classes. *J. Hazard. Mater.* **2009**, *171*, 739.

(24) Panofsky, H., Dutton, J. *Atmospheric Turbulence*; Wiley: New York, 1984.

(25) *FLUENT 6 User's Guide*; Fluent Inc.: Lebanon, NH, 2006.

(26) Ivings, M. J., Jagger, S. F., Lea, C. J., Webber,D. M. Evaluating Vapor Dispersion Models for Safety Analysis of LNG Facilities, *HSL Report*, 2007

(27) *PHAST 6.0 Technical Reference Manual*; DNV: London, U.K., 1999.

(28) Casada, M. L.; Nordin, D. C. The current status of LNG facility standards and regulations. *Proc. Safety Progress* **2005**, *24*, 152.

(29) Busini, V., Derudi, M., Rota, R. Heavy gas dispersion in presence of large obstacles: selection of the modeling tools; to be submitted for publication.

(30) Hissong, D. W. Keys to modeling LNG spills on water. *J. Hazard. Mater.* **2007**, *140*, 465.

(31) Vesovic, V. The influence of ice formation on vaporization of LNG on water surfaces. *J. Hazard. Mater.* **2007**, *140*, 518.

(32) Johnson, D. W.; Cornwell, J. B. Modeling the release, spreading, and burning of LNG, LPG, and gasoline on water. *J. Hazard. Mater.* **2007**, *140*, 535.

(33) *GAMBIT 2.2 Tutorial Guide*; FLUENT Inc.: Lebanon, NH, 2004.

(34) Blocken, B.; Stathopoulos, T.; Carmeliet, J. CFD simulation of the atmospheric boundary layer: wall function problems. *Atmos. Environ.* **2007**, *41*, 238.

(35) Pitblado, R.; Baik, J.; Raghunathan, V. LNG decision making approaches compared. *J. Hazard. Mater.* **2006**, *130*, 148.